EDITORS
Thomas M. Moses and Shane F. McClure
GIA Gem Laboratory

CONTRIBUTING EDITORS
G. Robert Crowningshield
GIA Gem Laboratory, East Coast
Cheryl Y. Wentzell
GIA Gem Laboratory, West Coast

DIAMOND

Fracture Filled, with Varying Results

Fracture filling is usually effective at making a diamond's fractures less obvious both to the unaided eye and when viewed with magnification, although a trained gemologist often can identify the treatment relatively easily. When the filling is not complete or is poorly executed, however, identification can be much more challenging. Two diamonds recently submitted to the East Coast laboratory highlighted these challenges.

The 9.01 ct rectangular modified brilliant in figure 1 was quickly identified as an artificially irradiated diamond, but as noted in the last issue of this journal (Spring 2005 Lab Notes, p. 46) identification of one treatment may not be the end of a gemologist's work. While the fractures in this diamond were generally quite visible, some contained an unusual texture and flow structure (figure 2) that led us to examine the stone more closely. A careful investigation at high magnification and with the light at varying angles revealed the telltale flash-effect colors associated with fracture filling.

We do not know exactly why the treatment was ineffective in this stone; however, a close look at figure 2 shows that the surface of the facet has a mottled, hazy appearance, which suggests that it may have been burned. Excessive heat can cause a high-lead glass filling to flow out of a fracture, and the dendritic patterns we observed (see also figure 3) support this possibility. One might further speculate that the excessive heat could have been generated during the color treatment process, since creating yellow color through artificial irradiation requires subsequent annealing. The heat necessary (~600°C) would certainly be sufficient to cause the filling material to break down. Thus, the fractures likely became much more visible than they were immediately after the fracture filling.

Another diamond, a 1.52 ct marquise, also had relatively obvious fractures that would not be expected in a clarity-enhanced stone. However, thorough examination with magnification revealed a very unusu-

Figure 1. This artificially irradiated 9.01 ct yellow diamond also showed unusual clarity enhancement features.

Figure 2. Heat treatment of the diamond in figure 1 may have created the unusual texture and flow structure visible within this fracture. Magnified 45x.

Figure 3. This dendritic pattern in another fracture in the 9.01 ct diamond indicates both the presence of a glass filler and exposure to high heat. Magnified 60x.

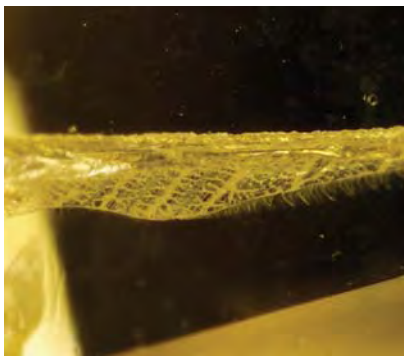

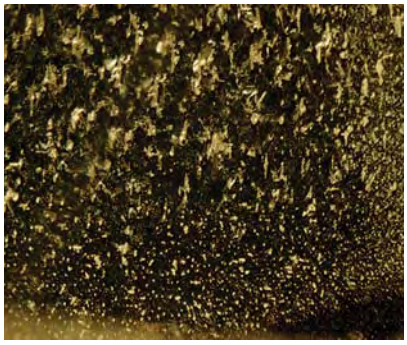

Figure 4. The unfamiliar pattern within this fracture led to closer examination of the 1.52 ct diamond for evidence of clarity enhancement. Magnified 75x.

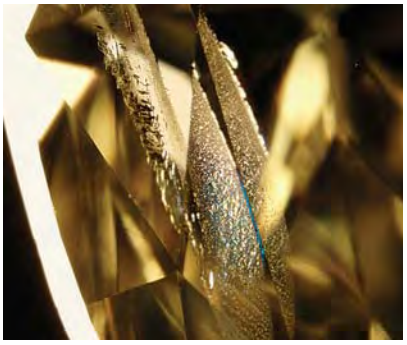

Figure 5. These subtle flash-effect colors in the 1.52 ct marquise are further indications of clarity treatment. Magnified 50x.

al pattern within the fractures (figure 4), which led us to look closely for more classic indications of clarity treatment. Figure 5 shows the very weak flash-effect colors that we found at higher magnification with the aid of fiber-optic illumination. Again, we do not know the exact reason for this poor result. However, there may have been a problem with the contact between the host diamond and the filler. These situations usually arise when the glass does not fill the entire fracture or it has been altered in some way due to either mishandling or possibly a "flaw" in the treatment process.

Diamonds such as these can create great challenges for the practicing gemologist. Anything unusual bears careful scrutiny, but with diligence the proper identification can often be made using the standard instrumentation available to most gemologists and jewelers.

Thomas Gelb and Matthew Hall

Editor's note: The initials at the end of each item identify the editor(s) or contributing editor(s) who provided that item. Full names are given for other GIA Gem Laboratory contributors.

GEMS & GEMOLOGY, *Vol. 41, No. 2, pp. 164–175*

Large Diamond with Micro-inclusions of Carbonates and Solid CO_2

Natural diamonds occasionally contain microscopic inclusions of carbonates, water, apatite, and silicates (see, e.g., O. Navon et al., "Mantle-derived fluids in diamond micro-inclusions," *Nature*, Vol. 335, 1988, pp. 784–789; Winter 2004 Lab Notes, pp. 325–326). These inclusions are encapsulated samples of mantle fluid, and thus are important for geochemical study of the mantle as well as for a better understanding of diamond formation. Although diamonds typically form at a depth of around 140–200 km, micro-inclusions of solid CO_2 were reported in a small rough type IaA diamond that is thought to have formed at a deeper origin, around 220–270 km (M. Schrauder and O. Navon, "Solid carbon dioxide in a natural diamond," *Nature*, Vol. 365, No. 6441, 1993, pp. 42–44). The discovery of solid CO_2 in diamond has very important implications in the study of the earth's mantle. However, that small crystal was the only specimen reported in which solid CO_2 micro-inclusions had been confirmed, except for a brief report of CO_2-bearing diamonds in a recent publication (T. Hainschwang et al., "HPHT treatment of different classes of type I brown diamonds," *Journal of Gemmology*, Vol. 29, 2005, pp. 261–273). Thus, the East Coast laboratory was very interested to examine a large faceted diamond that proved to contain micro-inclusions of solid CO_2 and carbonates, possibly from an even greater depth in the mantle.

The 5.04 ct pear-shaped diamond (14.94 x 9.26 x 6.27 mm; figure 6) of unknown geographic origin was graded D color. Although only a few very tiny pinpoint inclusions were visible with magnification, this stone displayed extremely strong colorless graining that created an undulating translucency throughout the entire diamond (figure 7). This severely affected its clarity, resulting in a grade of SI_2. Linear or planar graining occurred in a limited region close to the point of the pear shape. To the best of our recollection, the undulatory graining in this stone is the most prominent we have seen in the GIA Gem Laboratory.

The infrared spectrum (figure 8) showed no nitrogen- or boron-related absorption, which suggests that it is a type IIa diamond. This was supported by the ultraviolet (UV)-visible absorption spectrum, which did not show any absorption peaks. Unlike typical type IIa diamonds, this stone displayed a moderately strong yellow fluorescence

Figure 6. Spectroscopic analysis of this 5.04 ct D-color diamond revealed that it contains very unusual micro-inclusions of solid CO_2 as well as carbonates.

Figure 7. Hazy, undulatory graining is evident throughout the diamond in figure 6. This is the most intense graining seen so far in the laboratory, and it severely affected the diamond's clarity grade (SI_2). Image width is 8.0 mm.

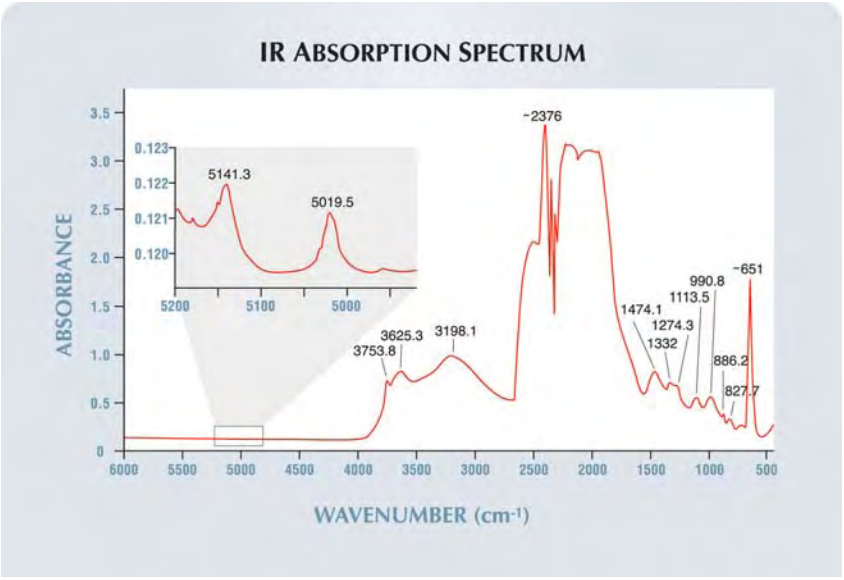

Figure 8. In the IR spectrum of the diamond in figure 6, strong absorptions of solid CO_2 occur at approximately 2376 and 651 cm^{-1}. Weak combination modes at 5141.3, 5019.5, 3753.8, and 3625.3 cm^{-1} also were observed; the weak absorptions at 1474.1 and 886.2 cm^{-1} are most likely from micro-carbonate inclusions.

to short-wave UV radiation. In the Diamond Trading Company (DTC) DiamondView, a moderately strong blue-gray fluorescence and weak blue-gray phosphorescence were observed; the undulatory appearance was also apparent (figure 9). Natural type IIa diamonds rarely phosphoresce.

The IR spectrum exhibited strong absorptions of fundamental modes of solid CO_2 at ~2376 (v3) and ~651 (v2) cm^{-1}. These two absorptions were so strong that their positions could not be precisely determined. Weak combination modes at 5141.3, 5019.5, 3753.8, and 3625.3 cm^{-1} also were observed. Close examination of these absorption positions and comparison with high-pressure spectral data of solid CO_2 revealed that the positions of these combination modes closely fit those seen in solid CO_2 under a pressure of 6.3 ± 0.4 GPa at room temperature (see R. C. Hanson and L. H. Jones, "Infrared and Raman studies of pressure effects on the vibrational modes of solid CO_2," *Journal of Chemical Physics*, Vol. 75, 1981, pp. 1102–1112). This pressure is higher than the 5 ± 0.5 GPa in the stone reported by Schrauder and Navon (1993). Extrapolation to a mantle temperature of 1,200°C results in a pressure of 9.2–9.7 GPa, about 270–290 km in mantle depth. These very likely represent the conditions under which the diamond originally crystallized. These pressure regimes are much higher than those in which most natural diamonds have grown (5–6 GPa), which further indicates that this diamond formed deeper in the mantle.

The weak absorptions observed at 1474.1 and 886.2 cm^{-1} (again, see figure 8) are most likely from micro-carbonate inclusions. These peak positions do not entirely fit with those of published calcite or magnesite positions at ambient conditions, and a pressure effect like that of solid CO_2 is highly possible. The weak absorptions at 1274.3, 1113.5, 990.8, and 827.7 cm^{-1} may be from other components that also occur as micro-inclusions. However, their assignment is not clear at this moment. Raman spectroscopy showed no Raman peaks for solid CO_2 or carbonates, but it did reveal many unusual photoluminescence emissions at liquid-nitrogen temperature using 488 nm laser excitation (figure 10). Except for the 3H emission at 503.5 nm, little is known about the assignment of other observed lines, which rarely occur in "standard" natural diamonds.

Figure 9. The undulatory graining seen in figure 7 is also apparent in the DTC DiamondView fluorescence image.

We believe the micro-inclusions and associated graining are the main cause of the undulatory hazy appearance. The micro-inclusions of solid CO_2 and carbonates in this gem diamond indicate a localized pocket of carbonate-rich material within the deep mantle (>200 km). Furthermore, this environment must have been stable for an extended period, allowing for the growth of this fairly large gem-quality diamond. This diamond represents the largest of those so far reported from the deep mantle. It is an unusual

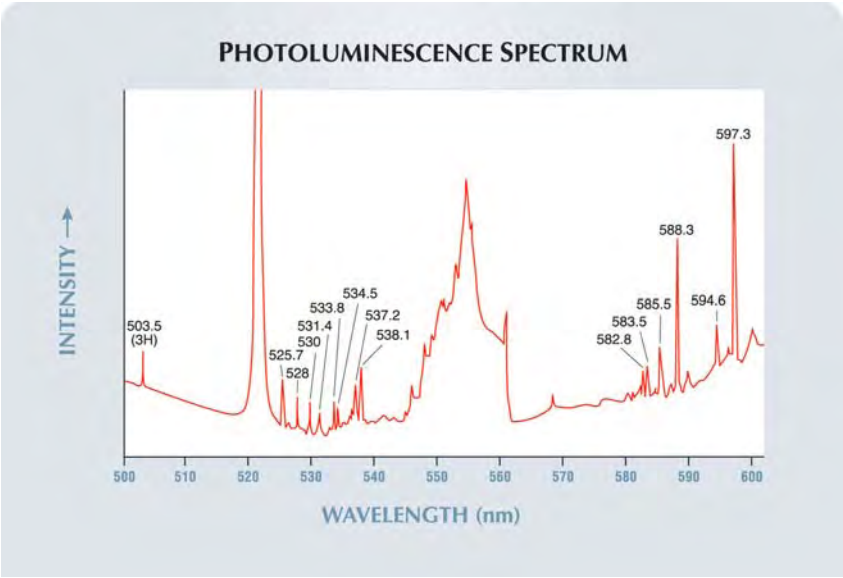

Figure 10. Except for the 3H emission at 503.5 nm, little is known about the assignment of the many photoluminescence emissions observed in the 5.04 ct diamond.

stone not only because of its special gemological properties but also for its importance in studying the earth's mantle and diamond formation.

Wuyi Wang, TM, Kyaw Soe Moe, and Andy Hsi-Tien Shen

Light Blue Diamond, with Type IIb and IIa Zones

Like some forms of nitrogen, boron occurs as individual atoms substituting for carbon in the diamond structure. However, boron and nitrogen typically do not coexist in natural diamonds. Unlike nitrogen-bearing diamonds and synthetic blue diamonds, which frequently exhibit distinctive growth zoning (best seen with the DTC DiamondView), most natural type IIb diamonds appear to have no—or only very subtle—zoning.

An interesting 0.67 ct light blue pear shape was recently submitted to the West Coast laboratory for grading (figure 11, left). Initial infrared absorption spectroscopy indicated that this diamond was type IIa, which suggested that the color was due to radiation-related defects. Low-temperature visible absorption spectroscopy, however, revealed the spectrum of a colorless IIa diamond with no evidence of radiation damage. The discrepancy between the spectroscopy and the light blue bodycolor led us to undertake a careful gemological examination.

The diamond was inert to long-wave UV radiation and fluoresced a very weak yellow to short-wave UV, with brief, very weak blue phosphorescence. When tested with a gemological conductometer, the stone showed slight electrical conductivity in certain directions. No color zoning was apparent when the pear shape was viewed with the microscope and diffused white light. Because in general these properties are consistent with type IIb diamonds, we decided to perform detailed UV imaging and collect spectroscopic data from different parts of the stone.

Phosphorescence in type IIb diamonds directly reflects the presence of boron, so we examined the diamond using the phosphorescence setup of the DiamondView to try to map the boron distribution. We were able to see small blue phosphorescent areas near the head and point of the pear shape that were not visible in the belly (figure 11, right). The degree to which the phosphorescent areas near the point represented boron enrichment is unclear, due to the tendency of pear-shaped brilliant cuts to collect color at the point. Our initial spectroscopic data had been collected by passing the beam through the girdle of the diamond at the belly; however, when the same measurements were taken near the head (where we saw the phosphorescent areas), the new absorption spectra revealed the presence of low concentrations of boron (figure 12). Although it is possible that hydrogen-boron complexes within the diamond may contribute to some of the observed features, the distinct differences in phosphorescence and the spectroscopic data collected from various parts of the stone strongly suggest that the diamond consisted of a mix-

Figure 11. This 0.67 ct Light blue pear-shaped diamond (left) was submitted for a colored diamond grading report. A DiamondView phosphorescence image (right) shows weak blue phosphorescence concentrated near the head and point of the pear shape.

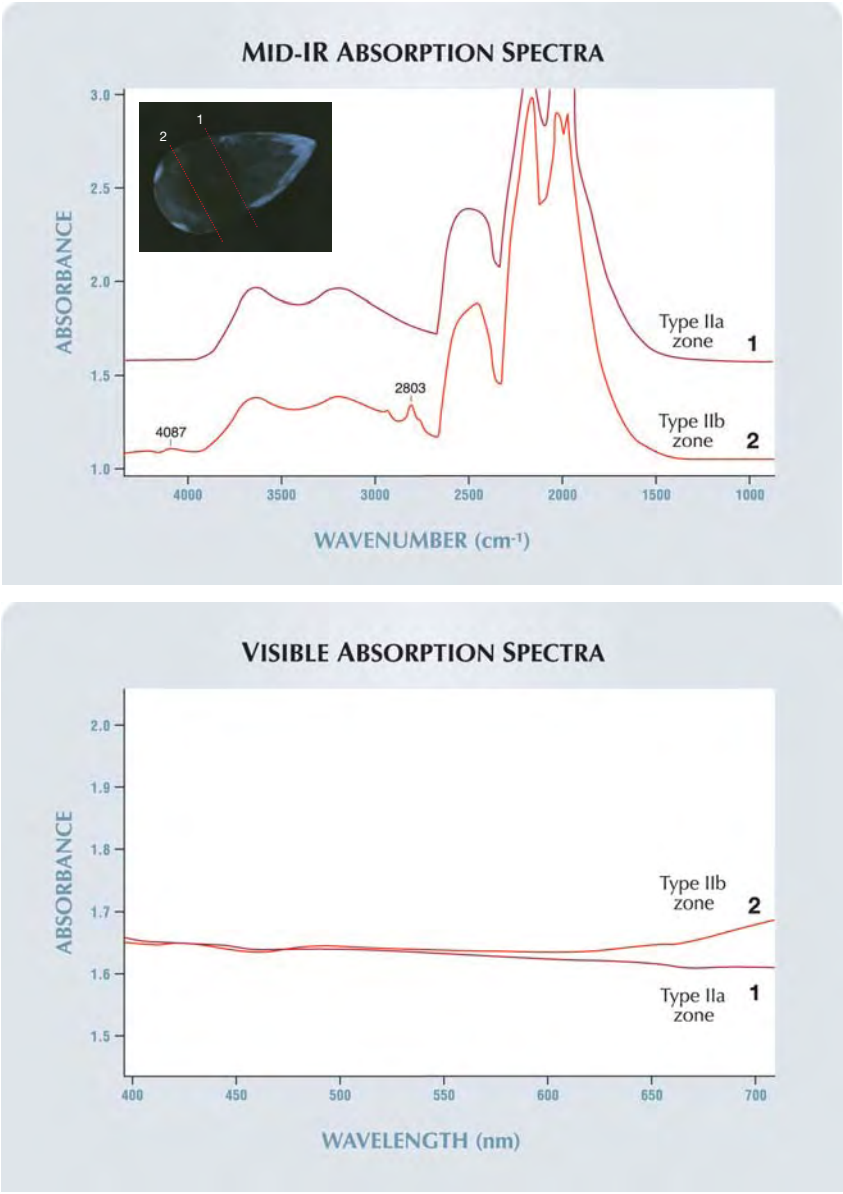

Figure 12. Mid-infrared (top) and visible (bottom) absorption spectra were collected from two different portions of the Light blue diamond, as indicated by the two lines in the phosphorescence image (top, inset). As would be expected from that image, the presence of boron is apparent only in the no. 2 spectra, as evident from the 2803 cm^{-1} IR feature and the increase in absorption at the red end of the visible spectrum (~600–700 nm).

ture of type IIa and IIb zones.

The Lab Notes section has published reports on a few other mixed type IIa and IIb diamonds (see Fall 1963, p. 85; Winter 1966–1967, p. 116; Fall 1993, p. 199; Summer 2000, pp. 156–157). Although spectroscopic data were not available from these reports, the nature of the type IIa/IIb zoning appears very similar to that of the diamond described here. This type of zoning in blue diamonds may be more common than we have believed.

Christopher M. Breeding

Natural Type Ib Diamond with Unusually High Nitrogen Content

Nitrogen is by far the most common impurity in diamonds. If most of the nitrogen in a diamond is present as isolated nonaggregated atoms within the crystal lattice (i.e., single substitutional N, or C-centers), the diamond is considered to be type Ib. Even very small amounts of this type of nitrogen (<10 ppm) can produce vivid yellow or orange-yellow colors, sometimes resulting in the highly sought-after "canary" diamonds (see, e.g., the article by J. M. King et al. on pp. 88–115 of this issue). Most natural type Ib diamonds contain less than 100 ppm of single substitutional N, though synthetic diamonds commonly contain much more. The concentration of C-centers in synthetic yellow diamonds typically ranges up to ~200 ppm, but may be even higher in deeply saturated yellow-orange or brown colors.

The West Coast laboratory recently had the opportunity to examine a natural diamond with unusually high Ib nitrogen content. The 0.24 ct Fancy Dark pink-brown oval cut shown in figure 13 contained so much nitrogen that the signal intensity in the region of the mid-infrared absorption spectrum where nitrogen is measured (the one-phonon region, ~1400–800 cm^{-1}) exceeded the limits of our detector. Higher-resolution data revealed that the diamond was mostly type Ib with

Figure 13. This 0.24 ct Fancy Dark pink-brown oval-cut diamond proved to have an unusually high type Ib nitrogen content.

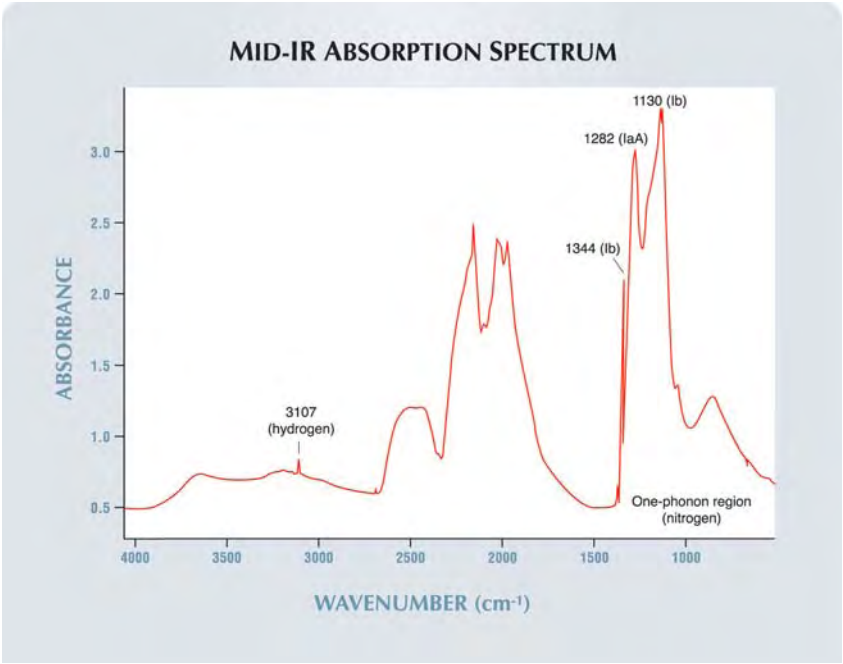

Figure 14. The mid-infrared absorption spectrum of the diamond in figure 13 displays peaks at 1344 and 1130 cm^{-1}, indicating a very high type Ib nitrogen content, as well as some type IaA nitrogen and small amounts of hydrogen.

Figure 15. The visible spectrum of the diamond in figure 13 shows complete absorption below ~515 nm and a broad band centered at ~610 nm; the latter probably contributes the pink component to the diamond's color.

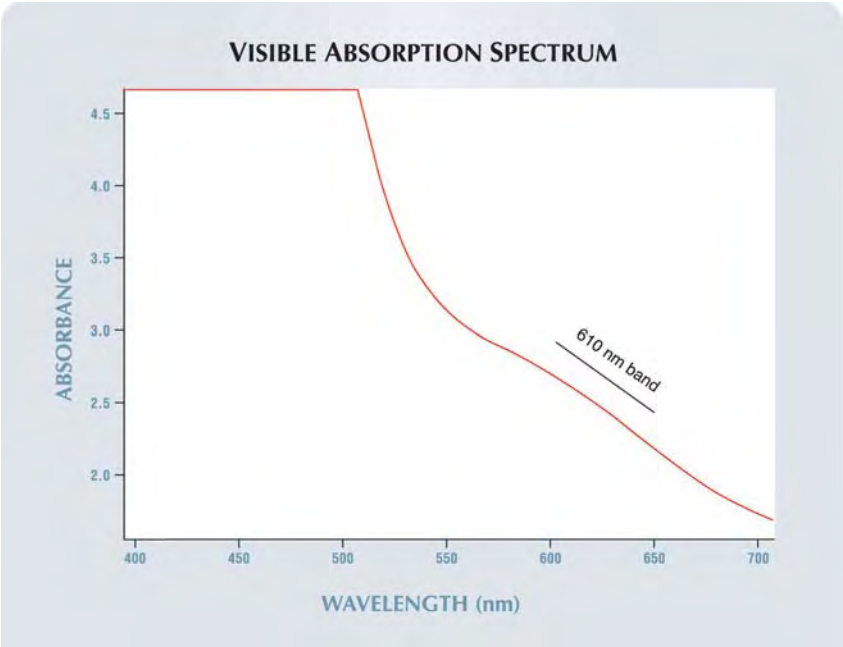

some type IaA (aggregated) N and also contained minor hydrogen (figure 14). Using FTIR software specially designed to measure nitrogen concentrations in diamond, we calculated levels of 364 ppm Ib nitrogen and 132 ppm IaA. This diamond contained more Ib nitrogen than any previous natural or synthetic diamond that we can recall examining in the laboratory. It is unusual that a diamond with such a high N content escaped aggregation and remained in its isolated form.

When examined with magnification, the diamond showed irregular color zoning and only a few small "feathers" and needle-like inclusions, similar to those we have previously seen in type Ib yellow diamonds (see, e.g., Spring 1994 Lab Notes, pp. 41–42; King et al., 2005). Strain was very weak and was localized around the inclusions. The diamond showed no reaction to either long- or short-wave UV radiation from a handheld lamp. In the desk-model spectroscope, general absorption was present below ~510 nm. More detailed data, collected at cryogenic temperatures using a high-resolution visible absorption spectrometer, revealed very strong absorption through most of the visible spectrum, with complete absorption below ~515 nm due to the abundance of Ib nitrogen (figure 15). The steady increase in absorption toward the blue end of the spectrum was accompanied by a broad band centered at ~610 nm that likely contributed the pink component of the face-up color. The origin of this band is unclear, but it may be an extension of the deformation-related 550 nm band that produces pink-red color in other natural diamonds.

The diamond was also examined with the DTC DiamondView. Several irregularly zoned areas of very weak green fluorescence were separated by more intense green boundaries. The zoning pattern of one region on the table was particularly interesting because it resembled the skeleton of a fish (figure 16). The reason for this unusual zoning pattern is not known at this time.

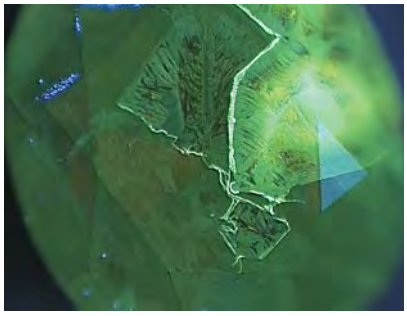

Figure 16. When exposed to strong short-wave UV radiation in the DTC DiamondView, the 0.24 ct pink-brown diamond shows zones that resemble the skeleton of a fish.

This stone is an excellent example of a rare and unique scientific treasure that belies its unremarkable appearance.

Christopher M. Breeding

Figure 17. This large cavity in an 8.38 ct diamond does not resemble any natural etch channels or laser drill holes seen previously in the laboratory. Magnified 35x.

With Unusual Laser Drill Holes

Over the past few years, the challenges posed by innovative diamond laser drilling techniques have increased markedly (see S. F. McClure et al., "A new lasering technique for diamond," Summer 2000 *Gems & Gemology*, pp. 138–146; Summer 2002 Lab Notes, pp. 164–165). Recently, a sharp-eyed diamond grader in the East Coast laboratory noticed something very strange in an 8.38 ct round brilliant and brought it to the attention of the Identification Department.

Our experience has been that laser drill holes are circular in appearance, while etch channels are angular, as they follow the diamond's crystal structure. The large cavities in this diamond (see, e.g., figure 17) were unlike any natural etching we have previously encountered. Yet, where they reached the surface, these "holes" were neither round nor angular; rather, their outlines consisted of numerous semicircles (figure 18). Long grooves, some of them with a black residue, ran down the length of the cavities (figure 19). These unusual striations mimicked what is characteristically seen in naturally occurring etch channels; if not scrutinized carefully, they could have been dismissed as natural inclusions.

Figure 18. Where the drill holes reach the surface of the diamond, they show an unusual outline, again unlike any previously encountered in the lab. Magnified 105x.

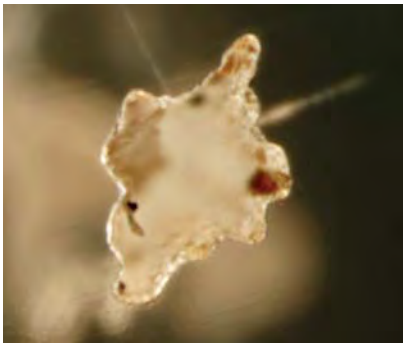

In this case, however, all of the questionable cavities tapered to solid inclusions (again, see figure 17). In addition, the grooves were rounded along their edges, and the dark color and sugary texture were reminiscent of laser drilling, which is known to leave a black residue. All of these clues led us to conclude that the cavities in this diamond were caused by laser drilling, perhaps the result of several holes drilled into the same area.

One could speculate that the drillers of this diamond were either trying to mimic natural etch channels or perhaps had outlined some near-surface crystals and drilled them completely out.

Joseph Astuto and Thomas Gelb

Yellowish Orange MAGNESIOAXINITE

The West Coast laboratory recently examined a 4.90 ct transparent brownish yellowish orange piece of rough (figure 20) that was submitted for identification by JOEB Enterprises of San Diego, California. This piece of rough, reportedly from Tanzania, was tabular in shape (17.75 x 8.86 x 3.64 mm) with parallel striations on some of its crystal faces.

Observation with a polariscope revealed a distinct biaxial optic figure.

Figure 19. Dark, rounded grooves along the length of this cavity in the 8.38 ct diamond are further indications of laser drilling. Magnified 45x.

Figure 20. This 4.90 ct piece of rough, reportedly from Tanzania, is the first known sample of yellowish orange magnesioaxinite seen in the GIA Gem Laboratory.

The material also displayed moderate yellow and orange pleochroism. A small flat that had been polished on the surface allowed us to obtain refractive indices of $\alpha = 1.657$, $\beta = 1.660$, and $\gamma = 1.668$, resulting in a birefringence of 0.011 and indicating that the optic sign was positive. The specific gravity, measured hydrostatically, was 3.18. The sample fluoresced moderate orange to long-wave UV radiation and weak orange to short-wave UV. Using a desk-model spectroscope, we observed only a broad absorption band from 450 to 520 nm. Examination with a gemological microscope revealed "fingerprints," fractures, needles, negative crystals, and distinct orange-yellow and near-colorless zoning. The identification of this sample did not appear to be straightforward on the basis of physical and optical properties alone, so we proceeded with more advanced testing.

Both Raman and X-ray powder diffraction analysis identified the material as a member of the axinite group. Axinite, $Ca_2(Fe, Mn, Mg)Al_2BSi_4O_{15}(OH)$, is a borosilicate mineral group made up of a solid-solution series with three end members: ferroaxinite, manganaxinite, and magnesioaxinite. The species designation depends on the relative amounts of iron, manganese, and magnesium, respectively. The R.I. and S.G. of the sample in question were almost identical to those reported for blue magnesioaxinite from Tanzania (E. A. Jobbins et al., "Magnesioaxinite, a new mineral found as a blue gemstone from Tanzania," *Journal of Gemmology*, Vol. 14, 1975, pp. 368–375). Puzzled by the fact that we were unable to locate any reference to magnesioaxinite with a yellowish orange color, we asked one of our research scientists to take the sample to Rutgers University in New Jersey for electron-microprobe analysis.

Analyses from three different spots indicated that the sample was chemically homogenous. Average results (reported in weight percent) were as follows: 46.74 SiO_2, below the detection limit for TiO_2, 18.39 Al_2O_3, 0.01 FeO, 0.80 MnO, 6.73 MgO, 21.53 CaO, 0.03 Na_2O, and 0.01 K_2O. This composition was consistent with that of the blue magnesioaxinite from Tanzania (see Jobbins et al., 1975; G. B. Andreozzi et al., "Crystal chemistry of the axinite-group minerals: A multi-analytical approach," *American Mineralogist*, Vol. 85, 2000, pp. 698–706). Vanadium was present as a minor constituent (0.13 wt.% V_2O_3) in the blue magnesioaxinite, and EDXRF analysis detected trace amounts of vanadium in the yellowish orange sample; unfortunately, quantitative microprobe data for vanadium were not collected.

In addition to the blue samples from Tanzania discussed above, brown-to-pink magnesioaxinite has been reported from Luning, Nevada. The material from Nevada has considerably less magnesium and more iron and manganese than the Tanzanian material (P. J. Dunn et al., "Magnesioaxinite from Luning, Nevada, and some nomenclature designations for the axinite group," *Mineralogical Record*, Vol. 11, 1980, pp. 13–15; Andreozzi et al., 2000). The Nevada samples contained just enough magnesium to fall within the broad magnesioaxinite range of the series, whereas the composition of the Tanzanian material was much closer to that of the pure magnesioaxinite end member. The difference in major-element chemistry between these two sources most likely explains their differences in color.

The brownish yellowish orange magnesioaxinite described here was similar in properties and chemistry to the blue Tanzanian material, which suggests that the yellowish orange color is probably not due simply to variations in iron, magnesium, and manganese. It is possible that variations in trace elements such as vanadium may contribute to the color, but as yet we do not know its true cause.

Elizabeth P. Quinn and Christopher M. Breeding

CULTURED PEARL
With Cultured-Pearl Nucleus

It is always exciting to discover the unexpected on a pearl radiograph. When the pendant in figure 21 arrived at the West Coast laboratory for a routine identification, we anticipated nothing unusual. However, the X-radiographs used in pearl analysis sometimes reveal surprises, and this proved to be one such specimen.

The baroque pearl measured 16.00 x 13.50 mm in width and depth. (We could not measure the length because

Figure 21. This 16.00 x 13.50 mm baroque cultured pearl contained an unusual surprise.

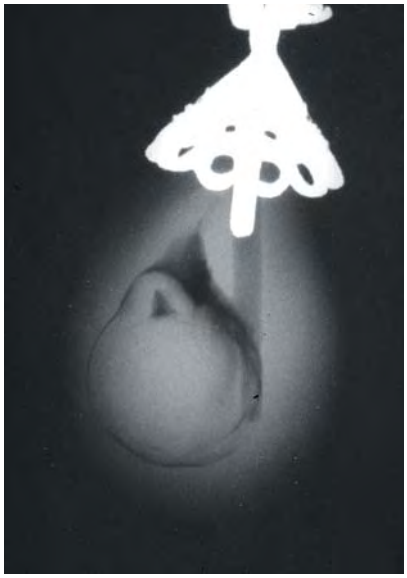

Figure 22. The X-radiograph of the cultured pearl in figure 21 revealed another cultured pearl as its nucleus, with bead and nacre clearly defined.

part of the pearl was covered by the mounting.) The X-ray luminescence was very weak, indicating that it might be a cultured pearl with thick nacre. However, X-radiography revealed that the nucleus did not merely consist of the expected mother-of-pearl bead, but it was in fact an *entire* cultured pearl with its own bead nucleus and nacre clearly defined on the radiograph (figure 22).

We have seen other cultured pearls with cultured-pearl nuclei; for example, we recently examined a semibaroque cultured pearl (approximately 18 ct) that appeared to contain a separate tissue-nucleated cultured pearl in its core (figure 23). The use of poor-quality cultured pearls as bead nuclei is a practice that has been known for a number of years, though it is unclear how common this practice is and we see very few such cultured-pearl nuclei in the laboratory. Nevertheless, gemologists relish having their routines broken by these small but delightful discoveries.

CYW

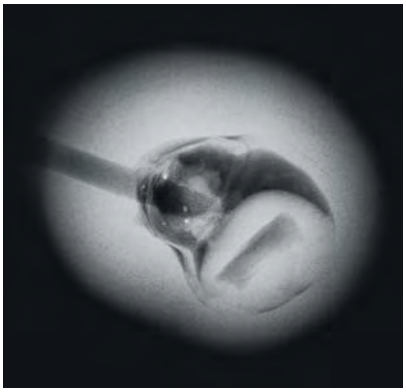

Figure 23. The ~18 ct cultured pearl in this X-radiograph appears to have a separate tissue-nucleated cultured pearl at its core.

Dyed "Golden" Freshwater Cultured Pearls

A graduated strand of what appeared to be "golden" South Sea cultured pearls arrived at the West Coast laboratory for identification (figure 24). We routinely examine these types of cultured pearls to determine whether or not they are dyed. This strand, however, provided another unexpected result.

Magnification revealed that the string knots between the cultured pearls were yellow, while the rest of the string was white. There also were concentrations of darker yellow around some of the drill holes (figure 25). These preliminary observations suggested that the color was artificial in origin. The reaction to long-wave UV radiation also was characteristic of treated-color pearls: Some fluoresced medium orangy yellow (occasionally mottled with blue), while others were medium pink with uneven orange mottling (figure 26). Naturally and uniformly colored yellow pearls evenly fluoresce yellow to greenish yellow or greenish brown to brown to long-wave UV; pink and orange components, along with blue patches and other mottling, are inconsistent with an evenly distributed natural color.

UV-Vis reflectance spectra were collected by research gemologist Shane Elen. The spectra consistently revealed a strong absorption trough in the blue region at approximately 415–440 nm rather than a deeper trough in the UV region at approximately 330–385 nm. These results are consistent with dyed yellow saltwater cultured pearls (see S. Elen, "Spectral reflectance and fluorescence characteristics of natural-color and heat-treated 'golden' South Sea cultured pearls," Summer 2001 *Gems &*

Figure 24. This strand of 34 dyed freshwater cultured pearls (approximately 10.60–11.70 mm) at first appeared to be typical "golden" South Sea cultured pearls.

Figure 25. Color concentrations around the drill holes of these freshwater cultured pearls, along with the yellow coloring on the knots of the string, indicate the presence of dye.

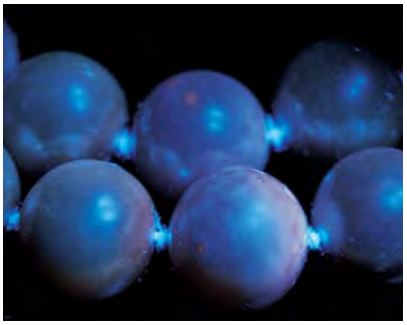

Figure 26. The mottled pink and orange long-wave UV fluorescence of these cultured pearls is consistent with treated color.

Gemology, pp. 114–123).

Treated-color yellow South Sea cultured pearls have become commonplace. The surprise with this necklace came while examining the X-radiographs. Rather than the expected bead nuclei, the radiographs revealed the characteristic structure of tissue-nucleated cultured pearls, immediately raising suspicion of freshwater origin.

EDXRF analysis (also performed by Shane Elen) confirmed a level of manganese that was consistent with a Texas freshwater pearl in the reference file. Mn can be found as a trace element in some saltwater pearls, but the amount present in these cultured pearls excluded the possibility of saltwater origin, thus proving they were freshwater cultured pearls that had been dyed to resemble "golden" South Sea cultured pearls. It is interesting to note that while the varied intensity (weak to strong) of the X-ray luminescence had supported the possibility of bead nucleation, it also was consistent with colored freshwater tissue-nucleated cultured pearls.

Although we do not have comparative UV-Vis spectra for dyed or natural-color yellow freshwater cultured pearls, the concentrations of color around the drill holes and unusual UV fluorescence behavior proved that these samples were dyed.

CYW

More on Copper-Bearing Color-Change TOURMALINE from Mozambique

The Fall 2004 Lab Notes section (pp. 250–251) reported on three unusual samples of copper-bearing tourmaline that displayed a strong and distinct "reverse" color change from grayish purple or purple in fluorescent light to gray–bluish green or gray in incandescent light (figure 27). We have now obtained quantitative chemical data on all three of these samples; after the table of the pear-shaped preform was polished (with the client's permission), the stones were analyzed by electron microprobe by Dr. William B. (Skip) Simmons and Alexander U. Falster at the University of New Orleans in Louisiana.

The analyses (table 1) show that the tourmalines are elbaite, with slight variations in composition. Their major-element compositions are comparable to those reported for cuprian elbaite from the Paraíba and Rio Grande do Norte states in Brazil (see, e.g., J. E. Shigley et al., "An update on 'Paraíba' tourmaline from Brazil," Winter 2001 *Gems & Gemology*, pp. 260–276). However, their Cu contents were significantly lower than those reported for "Paraíba" tourmaline: They ranged from below the detection limit (< 0.008) to 0.09 wt.% CuO. These values also are significantly lower than those reported for most of the cuprian tourmalines from Nigeria that have been analyzed (see Gem News International, Fall 2001, pp. 239–240, and Spring 2002, pp. 99–100).

Only minute amounts of Fe and Ti were detected in some analyses of each stone. Although EDXRF analysis had detected Ga and Bi (again, see the Fall 2004 Lab Note), these elements were below the detection limits of the electron microprobe. The traces of Pb measured in some analyses are consistent with those found in cuprian elbaite from other localities, and the client confirmed that no

Figure 27. These three color-change tourmalines, reported to be from Mozambique (viewed in fluorescent light at left and incandescent light at right), contain Mn and Cu as their primary chromophores. They weigh 5.37, 5.47, and 5.68 ct.

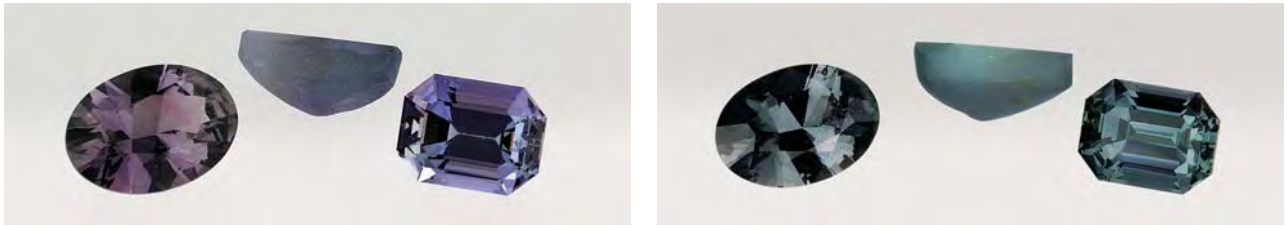

TABLE 1. Electron-microprobe analyses of three samples of color-change elbaite tourmaline from Mozambique.[a]

Chemical compostion	5.37 ct grayish purple oval	5.68 ct purple emerald cut	5.47 ct purple pear preform
Oxides (wt.%)			
SiO_2	36.61–36.77	36.61–36.86	36.69–36.87
TiO_2	0.01–0.04	bdl–0.01	bdl–0.01
B_2O_3[b]	10.98–11.00	11.01–11.06	11.03–11.12
Al_2O_3	41.53–41.76	42.51–42.77	42.53–42.79
V_2O_3	bdl–0.02	0.08–0.15	0.08–0.11
FeO	0.02–0.05	bdl–0.01	bdl–0.01
MnO	1.94–2.14	0.07–0.11	0.11–0.15
CuO	bdl–0.09	bdl–0.03	bdl–0.03
SrO	0.02–0.08	0.02–0.04	0.02–0.03
CaO	0.45–0.51	0.72–0.89	0.60–0.68
PbO	bdl–0.02	bdl–0.04	bdl
ZnO	bdl	bdl–0.03	bdl–0.04
Li_2O[b]	1.77–1.84	1.94–2.06	1.95–2.16
Na_2O	1.95–2.14	1.48–1.78	1.67–1.80
K_2O	bdl	bdl–0.04	bdl
H_2O[b]	3.35–3.39	3.33–3.37	3.32–3.36
F	0.84–0.95	0.94–0.99	0.97–1.03
Sum	99.98–100.31	99.13–99.78	99.32–99.69
-O=F	0.35–0.40	0.40–0.42	0.41–0.43
Total	99.60–99.91	98.73–99.36	98.89–99.25
Ions on the basis of 31 (O,OH,F)			
Si	5.796–5.817	5.769–5.789	5.764–5.791
Al	0.183–0.204	0.211–0.231	0.209–0.236
T sum	6.000	6.000	6.000
B	3.000	3.000	3.000
Al (Z)	6.000	6.000	6.000
Al	1.545–1.575	1.661–1.741	1.601–1.729
V^{3+}	bdl–0.002	0.011–0.018	0.009–0.014
Ti	0.002–0.004	bdl–0.001	bdl–0.001
Fe^{2+}	0.003–0.006	bdl–0.001	bdl–0.001
Mn	0.259–0.287	0.009–0.014	0.014–0.019
Cu	bdl–0.011	bdl–0.004	bdl–0.003
Sr	0.001–0.007	0.002–0.003	0.001–0.003
Pb	bdl–0.001	bdl–0.002	bdl
Zn	bdl	bdl–0.004	bdl–0.004
Li	1.126–1.173	1.233–1.302	1.239–1.361
Y sum	3.000	3.000	3.000
Ca	0.076–0.086	0.121–0.150	0.101–0.115
Na	0.598–0.658	0.452–0.543	0.509–0.548
K	bdl	bdl–0.008	bdl
Vacancy	0.256–0.326	0.309–0.426	0.340–0.391
X sum	1.000	1.000	1.000
F	0.422–0.475	0.468–0.491	0.480–0.511
OH	3.525–3.578	3.509–3.532	3.489–3.520

[a] *Analyzed with an ARL SEMQ electron microprobe, using an accelerating voltage of 15 kV, a beam current of 15 nA, a spot size of 2 μm, and 100-second count times for each spot. Ranges are shown for five points analyzed on each sample. Mg, Cr, Sc, Ga, Bi, and Cl were analyzed but were at or below the detection limit (except for 0.01 wt.% MgO in one analysis). Abbreviation: bdl = below detection limit.*

[b] *Values for B_2O_3, Li_2O, and H_2O were calculated based on an assumed elbaite tourmaline stoichiometry.*

lead-containing compounds were used in the cutting and polishing process. Thus, the speculation in the previous entry about Pb contamination from the polishing compound residue was probably erroneous.

The transition metals Mn, Fe, Ti, and Cu are the primary color-causing agents in tourmaline, in addition to V and Cr (W. B. Simmons et al., "Gem tourmaline chemistry and paragenesis," *Australian Gemmologist*, Vol. 21, 2001, pp. 24–29). The oval stone contained much more Mn than the other two samples. Its Mn content was comparable to that found in "Paraíba" tourmaline and similar to or slightly higher than that reported in cuprian elbaite from Nigeria (again, see Gem News International, Fall 2001, pp. 239–240, and Spring 2002, pp. 99–100). The emerald cut and pear-shaped preform had appreciably less Mn than has been reported in "Paraíba" tourmaline and in three violet-blue cuprian elbaites from Nigeria, but it fell within the lower range reported for four greenish blue Nigerian cuprian elbaites.

By correlating the chemical composition with the UV-Vis-NIR spectra of all three stones (figure 28), the particular chromophores and the color-change phenomenon can be better understood. Each stone had a broad absorption peak centered around 515 nm (attributed to Mn^{3+}). In addition, Cu^{2+} peaks were centered at approximately 690 and 900 nm ($E \perp c$), or 720 and 910 nm ($E \parallel c$). The latest data confirm our preliminary conclusion that manganese—specifically, Mn^{3+} residing in the Y crystallographic site—is one of the primary coloring agents of this material. Although the Cu concentrations are significantly lower than those of cuprian elbaites from Brazil and Nigeria, the presence of copper is also contributing to the color; however, the absorption caused by Mn^{3+} in these specimens most likely explains their less saturated and more purplish color in fluorescent light, along with the presence of some pinkish zones, as compared to the more intensely colored copper-induced blue hues of "Paraíba" tourmaline.

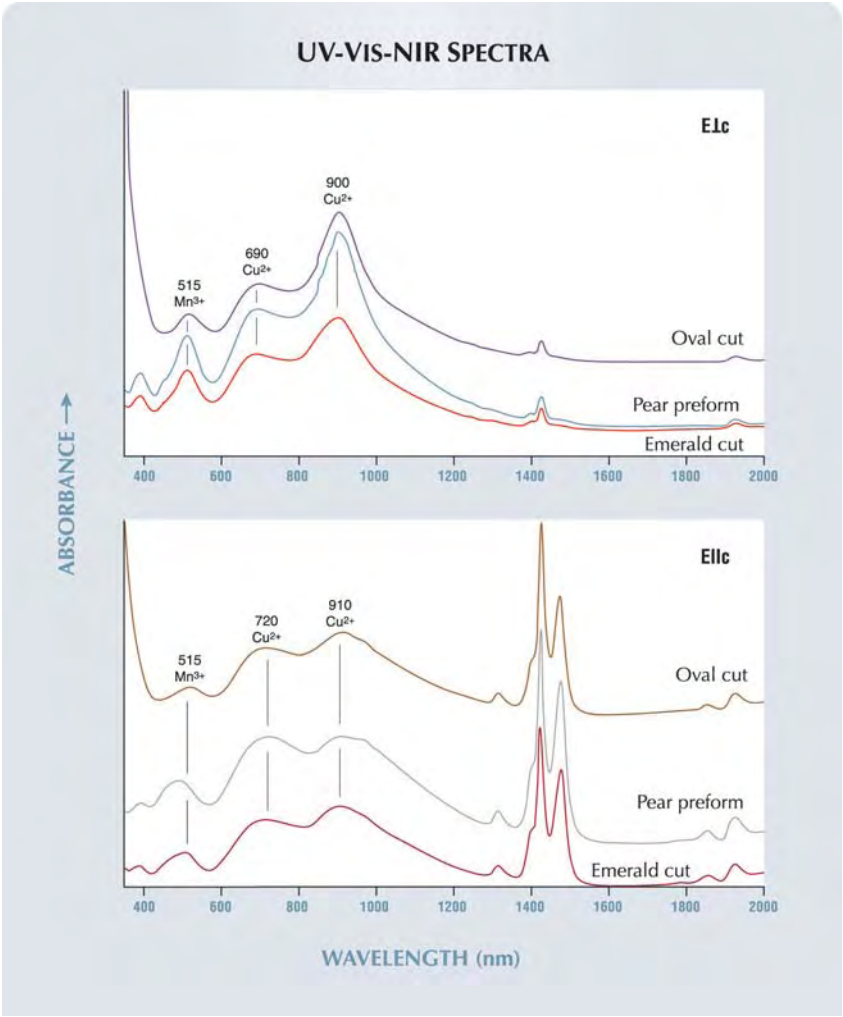

Figure 28. These polarized UV-Vis-NIR spectra for the three Mozambique tourmalines (E⊥c, top; E||c, bottom) show a broad absorption peak centered around 515 nm (attributed to Mn^{3+}), with transmission "windows" on either side centered at approximately 420–450 nm and 570–580 nm. These separate transmission maxima could account for the color-change phenomenon observed in these stones. The peaks from approximately 1400 to 1500 nm are due to OH^- groups. The inferred optical path lengths are as follows: emerald cut ~7 mm, pear-shaped preform ~8 mm, and oval ~6–8 mm. Spectra have been shifted vertically for clarity.

The color-change phenomenon may be explained by the transmission "windows" on either side of the Mn^{3+} absorption peak. These separate transmission maxima are centered at approximately 420–450 nm (the violet to "purple" spectral region) and 570–580 nm (the greenish yellow to yellow-orange region; again, see figure 28). However, often it is not possible to explain the observed color of a sample on the basis of the absorption spectra alone. Although the colors of our samples correspond to the approximate regions of maximum transmission in the absorption spectra, they do not correlate exactly; additional factors such as variables in the composition of the stones, lighting and viewing conditions, the manner in which color perception varies between individuals, and other considerations combine to determine the actual hues observed by each viewer (Y. Liu et al., "A colorimetric study of the alexandrite effect in gemstones," *Journal of Gemmology*, 1999, Vol. 26, No. 6, pp. 371–385). Thus, the exact cause of the reverse nature of the color change (relative to the "alexandrite effect") remains unknown. We are confident, however, that the unusual phenomenon could be further explained with a detailed colorimetric study in conjunction with the absorption spectra.

Although these Mozambique tourmalines were found to have much lower copper contents than their Brazilian and Nigerian counterparts, they do expand the geographic locales where copper-bearing elbaite has been found.

CYW, Eric Fritz, and Sam Muhlmeister

Although the concentrations of V were nearly equal to those of Mn in both the emerald cut and pear-shaped preform, and they exceeded the contents of Cu in the same stones, the absorption spectra do not show any indication of the V^{3+} peaks (599–610 nm and 418–440 nm) that have been reported for tourmaline (K. Schmetzer, "Absorption spectroscopy and colour of V^{3+}-bearing natural oxides and silicates—A contribution to the crystal chemistry of vanadium," *Neues Jahrbuch für Mineralogie, Abhandlungen*, Vol. 144, No. 1, 1982, pp. 73–106 [in German]); therefore, there is no evidence that V^{3+} is contributing to the color of these stones.

PHOTO CREDITS
Thomas Gelb—1–5, 17, 18, and 19; Jessica Arditi—6; Wuyi Wang—7 and 9; Maha Calderon—11 (left), 13, 20, 21, and 26; Christopher M. Breeding—11 (right) and 16; Cheryl Y. Wentzell—22 and 23; C. D. Mengason—24, 25, and 27.